2022
9(4), 364

Chemical Biology
LETTERS

Computational assisted designing, screening, and synthesis of novel inhibitor of malarial aspartic proteases plasmepsin I

Amit Kumar Gautam,[1] Rupini Boyina[2]

[1]*Department of Chemistry, D.A.V. (P.G.) College Kanpur-208001, U.P., India.* [2]*Deparment of Environmental Studies, SOITS, IGNOU, New Delhi-110068, India*

Received on: 28-Mar-2022 Accepted and Published on: 22-June-2022

Article

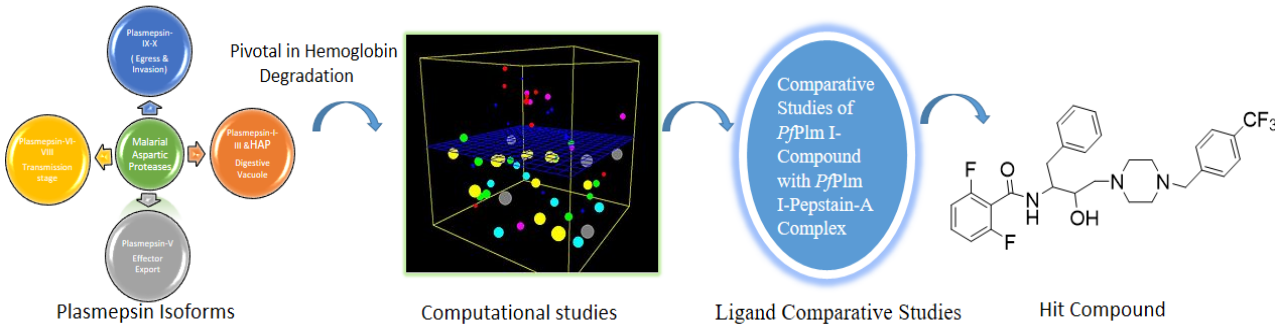

Aspartic protease enzymes of *Plasmodium falciparum* such as plasmepsin I (*Pf*Plm I) have been recognized as an interesting drug target for antimalarial drug discovery. For the immediate requirement of inhibitors of this enzyme, a computational approach was used to design HEA and piperazine analogs. We virtually screened 301 novel compounds based on validated pharmacophores *i.e.,* hydroxyethyl amine (HEA) and piperazine against *Pf*Plm I. The obtained hit compound in complex with *Pf*Plm I was subjected for molecular dynamics (MD) simulations at 200ns and found stable. Hit compound was further validated by wet lab experiments.

Keywords: Plasmepsin, Plasmodium, Proteases, Antimalarial drug, Analogs.

INTRODUCTION

Plasmodium falciparum (*Pf*) has four Plasmepsin (*Pf*Plms) inhabitants in their digestive food vacuole: *Pf*Plms I, II, IV, and Histo-Aspartic Proteinase (HAP).[1] These Plasmepsin are primarily interested in hemoglobin destruction, as evidenced by the commencement of hemoglobin hydrolysis by a pure naturally occurring enzyme. Despite the implementation of several malaria control initiatives around the world, substantial breakthrough in reducing new malaria cases has yet to be seen.[2] The Global Technical Strategy for Malaria 2016-30 expects a 90% reduction in clinical cases and deaths by 2030 compared to 2015.[3] However, due to parasite resistance to current antiparasitic drugs, including artemisinin, the current front-line treatment class,[4,5] these attempts are shown to be ineffective. Sequence wise about 53–70% amino acid similarities and a pattern of identical expression between *Pf*Plm I and its digestive vacuole plasmepsin paralogs matches.[6-8] *Pf*Plm I encodes a polypeptide with a lengthy prosegment of 123 amino acids and a mature part of 329 amino acids, as well as a putative transmembrane motif at the N-edge of the prosegment[8]. Based on sequence similarities between it and *Pf*Plm II and *Pf*PlmIV,[9-12] a bilobal tertiary structure analogous to Pepsin appears to evolve for the mature *Pf*Plm I. *Pf*Plm I is carried to the double membrane of the parasite surface, from where it is transferred to the digestive vacuole together with digested hemoglobin in conjunction with the maturation of zymogen to enzyme[13], according to research on immunolocalization of intraerythrocytic trophozoites. Pepstatin A, an aspartic proteinase inhibitor, and SC-50083, a potent inhibitor of *Pf*Plm I, both exhibit a similar ability to destroy cultured *P. falciparum* parasites, apparently through preventing hemoglobin breakdown.[14-15] Ro40–4388 and Ro40–5576 have antiparasitic action akin to Ro40–4388, a highly specific inhibitor of *Pf*Plm I.[16] Based on these sources of evidence, *Pf*PlmI may be the superior choice in the process of developing new malarial drugs. Several studies have shown that hydroxyethyl amine (HEA) and piperazine are effective PfPlm[17-19] binders. These results led us to synthesize HEA and piperazine analogs.

*Corresponding Author: Prof. B. Rupini, SOITS, IGNOU, New Delhi.
Tel: +91-9911223373 Email: brupini@ignou.ac.in

URN:NBN:sciencein.cbl.2022.v9.364
 ISSN: 2347–9825
https://pubs.thesciencein.org/cbl

METHODOLOGY

Protein preparation

RCSB protein databank (PDB) was consulted for the crystal structure *Pf*Plm I (PDB: 3QRV). The Protein Preparation Wizard including Schrodinger suite (Prime module) were adapted to prepare protein structure to rectify errors of structural exclusion pertaining to alternation conformation crystallographic water, missing atom's cation, and protonation with residues at the physiological pH[20]

Preparation of molecular library for virtual Screening

Pepstatin A (PubChem ID: 5478883) inhibits *Pf*Plm I, according to a prior study, and their structure files were retrieved from Pubchem.[21,22] Pepstatin A was used as a control in this investigation. Using the MAESTRO tool,[23] a library of 301 compounds was created based on the HEA and piperazine pharmacophore. HEA-based molecules have a number of advantages, including simple, large-scale production and the potential to treat a variety of diseases.[24-26] Ligprep[27] constructed the structure of Pepstatin A as well as the library of HEA and piperazine-based analogs prior to molecular docking. All parameters were left at their default values, with the exception of the chirality parameters for protease inhibitors and developed analogs. Both Pepstatin A and created analogs have their chiralities preserved (the SS conformer was specially chosen for the HEA collection) (Figure 1). All ligands were desalted, and tautomer were generated. Ionization states at pH 7 ± 2 for all compounds were estimated by the execution of the inbuilt Epik module of Schrodinger suite.[28]

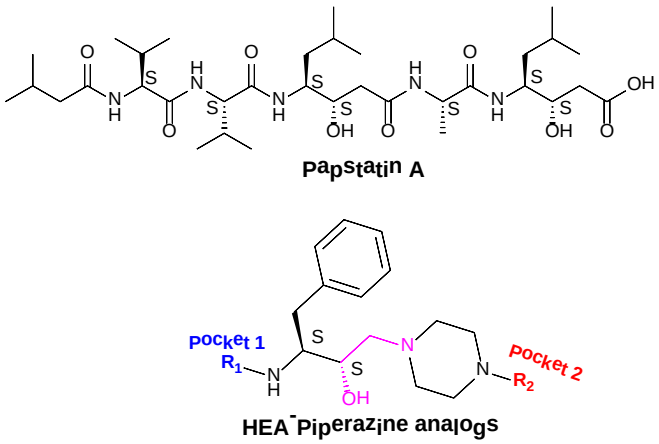

Figure 1: Stereo-geometry of Pepstatin A and HEA-piperazine analogs

Molecular docking studies

The Glide module[29] was practiced to earn site-specific molecular docking of Pepstatin and developed analogs against *Pf*Plm I. Using Glide, a receptor grid was created with default parameters, with van der Waals radii of 1.0 and 0.25 for scaling factor and partial charge cutoff, respectively. X=32.10, Y=33.15, and Z=12.47 were the grid center coordinates. The cubical grid box was a size 30. The molecular docking procedure was carried out with extreme precision (XP). A cutoff docking score value of -8.0 kcal/mol was used to filter the library. Pepstatin A, top-ranked compound's binding free energy was also calculated by prime MMGBSA.[30]

Molecular dynamics simulations

Molecular dynamic simulation was accomplished for selected docked complexes along with the selected control to learn about the dynamic behavior of the complexes. The simulations were carried out using the academic Molecular Dynamics tool Maestro Desmond with OPLS-2005 force fields[31-34]. TIP3P water model was used to solve the docked complexes in a 10×10×10 $Å^3$ orthorhombic box before simulations began[35]. The cation (Na^+) and anion (Cl^-) were added to neutralize the system and sustain the physiological pH. All systems were energetically optimized for 100ps at default settings prior to bifurcations. The Martyna–Tobias–Klein and Nose–Hoover chain dynamic algorithms were employed to maintain the optimal physical conditions for temperature at 300 K and pressure at 1.0 bar respectively.[36,37]

Following that, both docked systems were placed through a 200-ns production run. The stability of docked complexes was evaluated using a list of functions, including root-mean-square-deviation, root-mean-square-fluctuation with protein-ligand interactions, and contacts. Procheck[38] was used to assess the stereochemical geometry of *Pf*Plm I after MD simulation.

Validation of docking studies

Top-notched compounds based on glide docking score and XPGS score site-specific glide docking were allowed to re-screen using Autodock Vina in PyRx (version 0.8) as a docking validation method[39]. Before blind dockings, PyRx employed the universal force field and the adjoined algorithm to minimize all compounds. The pymol platform (The PyMOL Molecular Graphics System) was used to examine the results[40]. In non-site-specific docking investigations, the protein structure generated in silico after ligand removal was used.

Absorption, distribution, metabolism, and Excretion calculation

The Swiss ADME method was practiced to examine biological processes such as absorption, distribution, metabolism, excretion, and toxicity profile of potential compounds[41]. Molecular weight, rotatable bonds, HBA, HBD, TPSA, and projected octanol/water partition coefficient (MLogP), solubility (ESOL class), GI absorption, BBB permeant, P-glycoprotein substrate, cytochrome inhibitor (CYP1A2, CYP2C19, CYP2C9, CYP2D6, and CYP3A4), Lipinski inhibitor (CYP1A (drug-likeness).

Synthesis of compound

Briefly, 3.8 mmol of (2R,3S)-N-Boc-3-amino-1,2-epoxy-4-phenylbutane (**I**) and 1-(4-tri-fluoromethylbenzyl)piperazine (3.8 mmol) were taken into a 50 mL round-bottomed and dissolved in 5 mL of ethanol, and under the influence of microwave irradiation for a span of 30 minutes at 300W/80 reaction mixture was stirred (Figure 2). The solvent was extirpated under a vacuum after the reaction mixture attained room temperature. Ethyl acetate and hexane (1:9) were used to

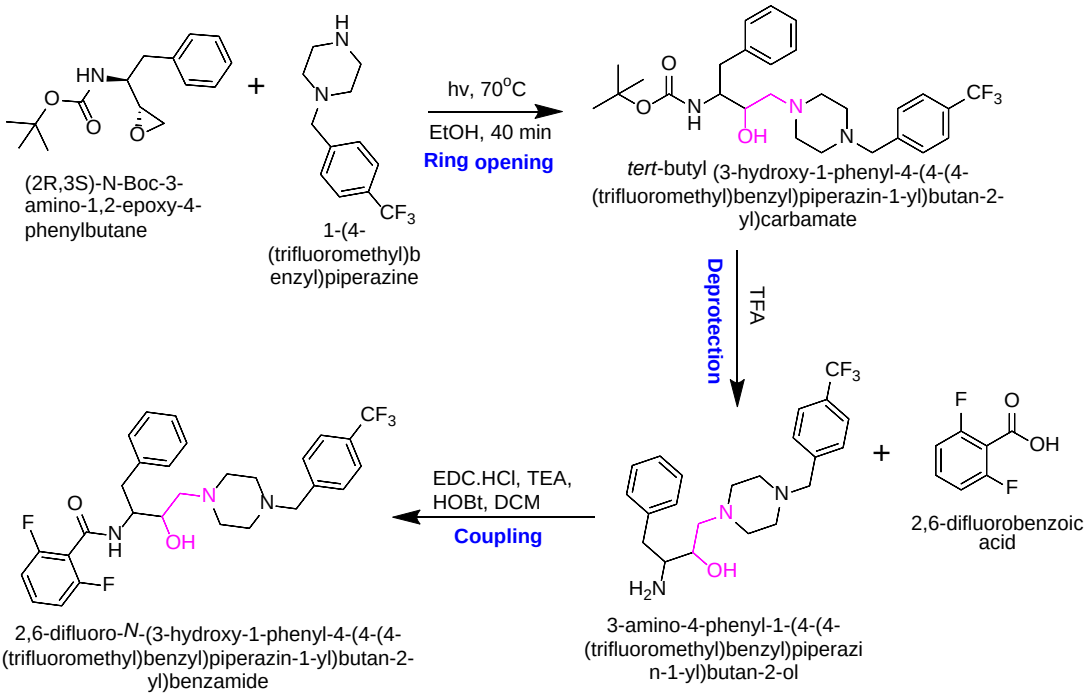

Figure 2: Schematic route for the synthesis of hit compound

recrystallize the crude product to be utilized for the further steps. The BOC deprotection was consummated in the subsequent step in a 100 mL flask, with contamination of the preceding step compound in dichloromethane with a 20 mL volume and added with trifluoracetic acid (3 mL, 15% of DCM) in a slow manner. At room temperature, stirring of the reaction mixture was carried out and surplus DCM and TFA were knocked off under vacuum after completion of reaction. 1M NaOH was used to adjust pH of the reaction mixture to 8-9 and ethyl acetate (4x30 mL) was utilized for the extraction process and a wash with brine solution (4x20 mL) was given. Finally, anhydrous sodium sulfate was added to make organic layer water-free and to afford the deprotected intermediate, excess of ethyl acetate was knocked off under reduced pressure. The mixture of 2,6-difluorobenzoic acid (1.5 mmol) and triethylamine (TEA) (4.5 mmol) in DCM (20mL) was stirred for a span of 30 min at the room temperature and subsequently addition of 1-Ethyl-3-(3-dimethyl aminopropyl)carbodiimide (EDC·HCl) (3.0 mmol) was effected. After 30min added hydroxyl benzotriazole (HOBt) (3.0 mmol) at 0°C with constant stirring for 30 mins and added deprotected intermediate (1.0 mmol). Extraction of the ultimate compound was executed with ethyl acetate (3x25 ml) after the reaction was finished and the excess amount of DCM was eliminated under vacuum. Anhydrous sodium sulfate was inevitably added to make organic layer water free, and solvent was eliminated, and purification of the final product was executed by means of column chromatography (70: 30, hexane: ethyl acetate).

Spectroscopic data for compound 1: 2,6-difluoro-N-(3-hydroxy-1-phenyl-4-(4-(4(trifluoromethyl)benzyl)piperazin-1-yl)butan-2-yl)benzamide : ^{1}H-NMR (400 MHz, $CDCl_3$) δ 7.77 – 7.51 (m, 4H), 7.48 – 7.25 (m, 5H), 7.23 – 7.16 (m, 3H), 4.69 (m, 1H), 4.17 (dt, *J* = 14.3, 7.4 Hz, 2H), 3.81 – 3.68 (m, 1H), 3.58 (s, 2H), 3.21 – 2.61 (m, 10H). ^{13}C NMR (100 MHz, $CDCl_3$): δ 174.32, 142.45, 138.30, 138.10, 129.56, 129.33, 129.25, 128.76, 128.47, 126.83, 126.52, 125.29, 125.26, 66.09, 62.40, 60.73, 56.72, 53.13, 51.52, 40.99, 39.02.

RESULTS AND DISCUSSION

Malaria is one of the deadliest diseases caused by *P. falciparum*. Targeting of *Pf*Plm I has significant effects on parasite survival as hemoglobin degradation is very essential for their survival[1-42]. Designed analogs may inhibit *Pf*Plm I activity leads to parasite growth inhibition. This finding encouraged us to design and screen analogs against *Pf*Plm I using computational approaches.

Molecular docking studies

Molecular docking calculations were accomplished in the pursuit of HEA-piperazine analogs using the GLIDE module that can robustly bind within *Pf*Plm I enzyme's active site bind. Docking score (kcal/mol) and glide XP Gscore are weighed to rank the ligand's poses banking on their binding affinity. All the 301 molecules docked within the binding pocket of *Pf*Plm I. The docking score and XP Gscore of Pepstatin A were observed as -1.734 kcal/mol, and -1.736 kcal/mol, correspondingly (Table 1, entry 2). A total of 49 compounds showed docking score better than cutoff score (-8.0 kcal/mol) whereas hit-compound possessed the highest docking score of value -8.617 kcal/mol (Table 1 entry 1 and Table 2 entry 1-48). Hit compound showed a XPG score (kcal/mol) together with binding free energy (kcal/mol) of -8.807, and -76.38, respectively (Table 1, entry 1) which significantly better than Pepstatin A. Finally, both hit-

compound and PepstatinA in complex with *Pf*Plm I were selected for further interaction analysis.

2D-docked interaction studies

Interaction plots as reflected in 2D-3D diagram for the docked candidates (Figure 5). Hit compound interacted to Tyr75, Asp215, and Phe117 while Pepstatin A interacted to residues Tyr75, Gly217, and Ser219 (Figure 5). Hit-compound interacted to catalytic residue Asp215 by H-bond and salt-bridge. Residues Tyr75 and Phe117 interacted to compound by H-bond and pi-pi interaction, respectively (Figure 5a). In *Pf*Plm II-Pepstatin A complex (Figure 5b), Pepstatin A interacted to residues Tyr75, Gly217, and Ser219 by H-bond interaction where Ser219 acted as HBD while Gly217 and Tyr75 acted as HBA.

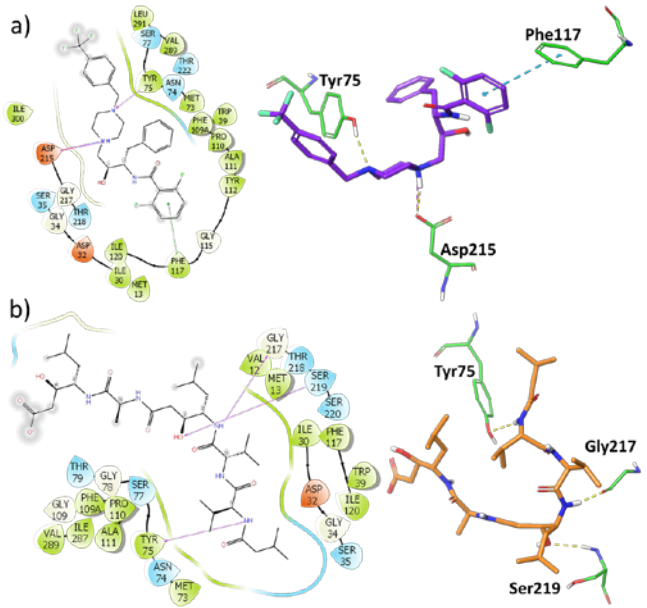

Figure 5: 2D-3D ligand interaction diagram showing ligand interacted to binding site residues; a) *Pf*Plm I-**hit compound** complex, **b)** *Pf*Plm I-PepstatinA complex

Molecular dynamics simulations

To evaluate the characteristics like stability, and behavior in conformational domain performance of molecular dynamic simulation was done for all top-ranked compounds and Pepstatin A with the selected *PfPlm* I. Calculation of the protein and ligand RMSD, RMSF, and contacts formed in the course of the simulation run presented stable behavior of the docked candidates. Both *Pf*Plm I- **hit Compound**, and *Pf*Plm I-Pepstatin A complexes were shortlisted for MD simulation at 200 ns.

Change in Root Mean Square deviation for protein Cα during the course of simulations was measured as a stability parameter of these system. The RMSD plot of Cα-*Pf*Plm I in complex with hit-compound, and Pepstatin A attained stability within first 5-10 ns and fluctuations were in acceptable region (<3Å) (Figure 6a,b). The average values of $RMSD_{C\alpha}$, and $RMSD_{backbone}$ for the *Pf*Plm I in complex with compound were 2.279Å and 2.276Å, respectively. Otherside average values of $RMSD_{C\alpha}$, and $RMSD_{backbone}$ for the *Pf*Plm I in complex with Pepstatin A were 2.675Å and 2.665Å, respectively. In both complexes, $RMSD_{backbone}$, and $RMSD_{C\alpha}$ were in the range from 2.0Å to 3.0Å. In all complexes *Pf*Plm I had similar average RMSD Cα, and backbone indicated protein was very stable in all systems and compounds were not causing any significant protein structural change.

In the next step, Ligand-RMSD and RMSF calculations were performed to confirm that ligand was stable within the binding pocket of *Pf*Plm I protein's binding pocket. The hit-compound achieved conformational stability nearby 15ns and average ligand RMSD was below 5.19Å while 7.66 Å for Pepstatin A (achieved stability nearby 75ns)**.** Both hit-compound and Pepstatin A deviated (after stability achieved) in the range from 4.275 Å to 6.089 Å and 6.411 Å to 8.932 Å, respectively. It clearly displayed in the ligand-RMSD (ligand fit on protein) plot, both molecules fluctuated by < 3Å (Figure 6a,b). The ligand RMSF plot for the ligand marked the ligand fluctuations in relation to the residues in the binding pocket, as well as the ligand atom contact with the solvent in the pocket.

Hit-Compound seemed very stable over Pepstatin A as there was low local fluctuation than Pepstatin A (Figure 6c,d). The change in ligand RMSD for hit-compound and Pepstatin A due to their respective moieties was also supported by ligand RMSF (Figure 6a-d).

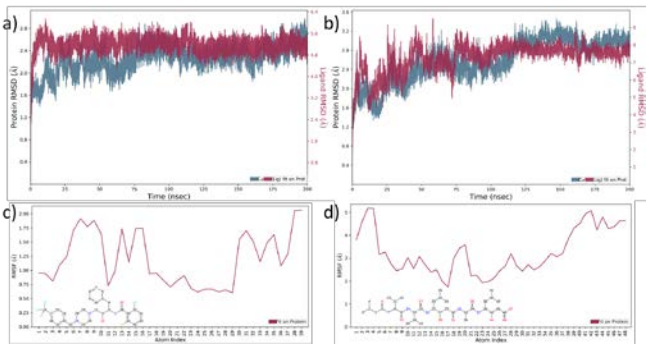

Figure 6: RMSD plot: **a)** *Pf*Plm I-**hit** complex, **b)** *Pf*Plm I-PepstatinA complex; Ligand RMSF plot: **c)** compound **hit compound**, **d)** PepstatinA

Hit-Compound interacted to both catalytic residues Asp32 and Asp215 by H-bond and salt-bridge during MD simulation along with several hydrophobic interactions, respectively (Figure7a). The PepstatinA also interacted with Asp32 but there were several water bridge interactions which may be responsible for conformational change in PepstatinA. This was also supported by ligand RMSD and ligand RMSF plot (Figure 6 and 7). The stereochemical geometry of *Pf*Plm I in complex with hit-compound and PepstatinA were also calculated by Procheck (Figure 7). Both complexes *Pf*PlmI-hit-compound and *Pf*PlmI-PepstatinA possessed only 0.3% and 0.7% residues in outlier region (Figure 8, Table 3 entry 1-2).

Docking Validation by non-site-specific docking

Our findings were also validated with non-site-specific docking (PyRx software) which showed hit-compound occupied

binding site only (Figure 9) which indicated, there was no allosteric site for hit-compound.

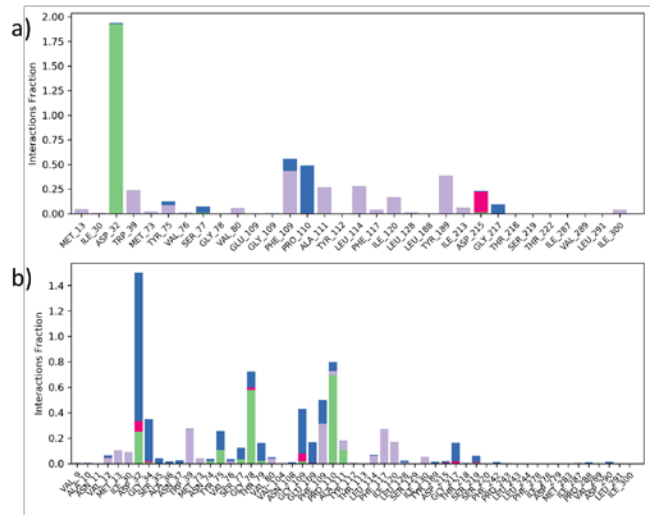

Figure 7: Ligand contacts histogram: **a)** *Pf*Plm I-**hit** complex, **b)** *Pf*Plm I-PepstatinA complex**.**

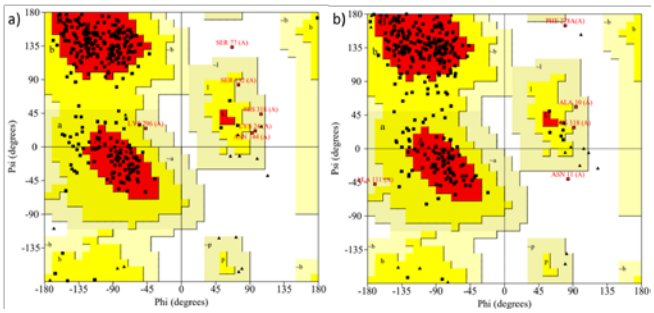

Figure 8: Ramachandran plot: **a)** *Pf*Plm I-**hit**-complex, **b)** *Pf*Plm I-**Ct** complex

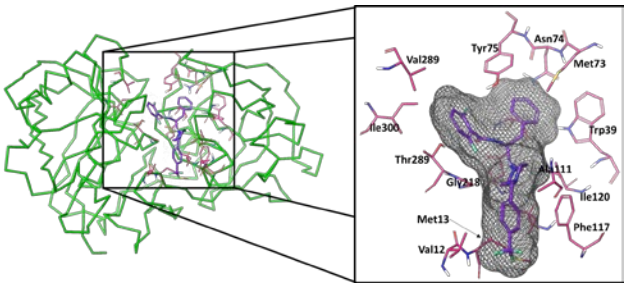

Figure 9: Docking validation by non-site-specific docking

Absorption, Distribution, Metabolism, Excretion properties

The ADME profile was calculated through Swiss-ADME for compounds. Hit-compound showed H-bond donors, molecular weight (g/mol), MLogP, and H-bond acceptors of 2, 547.56, 4.43, and 9, respectively. All of them have TPSA score of 55.81 $Å^2$ and moderate solubility in water. They have shown high GI absorption and may permeate blood-brain barrier (BBB) also. All of them have a nature of Pgp substrate as well as do not inhibit cytochrome CYP1A2, CYP2C19, and CYP2C9 except Cyp2D6 and Cyp3A4. Hence hit-compound needed to be validated by wet-lab experiment**.**

Structure-Activity Landscape Index (SALI) Similarity Map Compounds in complex with *Pf*Plm I

Initially, the pocket-I having 2,6-difluoro benzoic acid was kept constant and the substitutions made at pocket-II that linked to piperazine moiety. A pool of 9 distinct compounds (Figure 10) compound **1–9** (Table 4, entry 1–9) were ranked for docking score with alteration at pocket II. The compounds **1-9** containing different functional groups at pocket 2 such as 4-(trifluoromethyl)benzyl, 2-methylbenzyl, tert-butylbenzyl, 2,5-difluorobenzyl, 3-(trifluoromethyl)benzyl, 4-methylbenzyl, phenyl, benzyl, and benzhydryl were shown to own inflated docking scores in analogy to **Ct** but only compound **1-3** showed better docking score than cutoff (-8.0 kcal/mol). During SAR analysis of compounds in which pocket I was kept constant, two pairs of compounds **1** and **3** having similarity by 98% while compound **2** and **8** showed structural similarity by 97% as depicted in (Figure 10). However, docking score between **1**(-8.617 kcal/mol) and **3** (-8.27 kcal/mol) varied due to $–CF_3$ group (compound **1**) and -tert-butyl group (compound **3**). The presence of electron-withdrawing group (EWG) at para position showed a significant effect on docking score when compared to compound 3 having electron-donating group as para position (-tert-butyl group). EWG at meta and ortho also showed better docking score when compared to compound **4** (-7.942 kcal/mol) having 2,5-difluorobenzyl group and compound **5** (-7.776 kcal/mol) having 3-trifluoromethylbenzyl piperazine. Similarly, EDG at meta position in compound **2** (-8.592 kcal/mol) showed significant effects on docking score when compared to EDG at para position in compound **3** (-8.27 kcal/mol) and compound **6** (-7.646 kcal/mol). Docking score was significantly influenced during performance by electron-withdrawing group over electron-donating group.

In the following pursuit, changes were made at pocket-1 while preserving the 4-(trifluoromethyl)benzyl group constant at pocket-II then 29 distinct functionalities (Figure 11) were shortlisted (Table 4, entry 1 and 10-37). Out of the 29 compounds, an elevated docking score compared to hit-compound was not detected for anyone. Similarly, SAR analysis of compounds having constant pocket II, showed five groups of compounds having structural similarity of >95% such as compounds [**1** and **17]**, [**15** and **27]**, [**20** and **30]**, [**32** and **37]**, and [**10, 12, 13, 16, 24, 25, 29,** and **34]**. During this analysis, results were observed that compound **17** (-7.855 kcal/mol) having 2-bromo-6-iodobenzyl group showing Br and I at both ortho positions showed a low docking score compared to hit-compound (-8.617 kcal/mol) having strong EWG at both ortho positions which indicated significance of strong EWG at both ortho position instead of less EWG. The compound **15** (-7.962 kcal/mol) having high docking score than compound **27** (-7.256 kcal/mol) suggested that halide group having low electronegativity at *para* position has significant effects on docking score over halide group having high electronegativity at *para* position. It was also observed that strong EDG at para

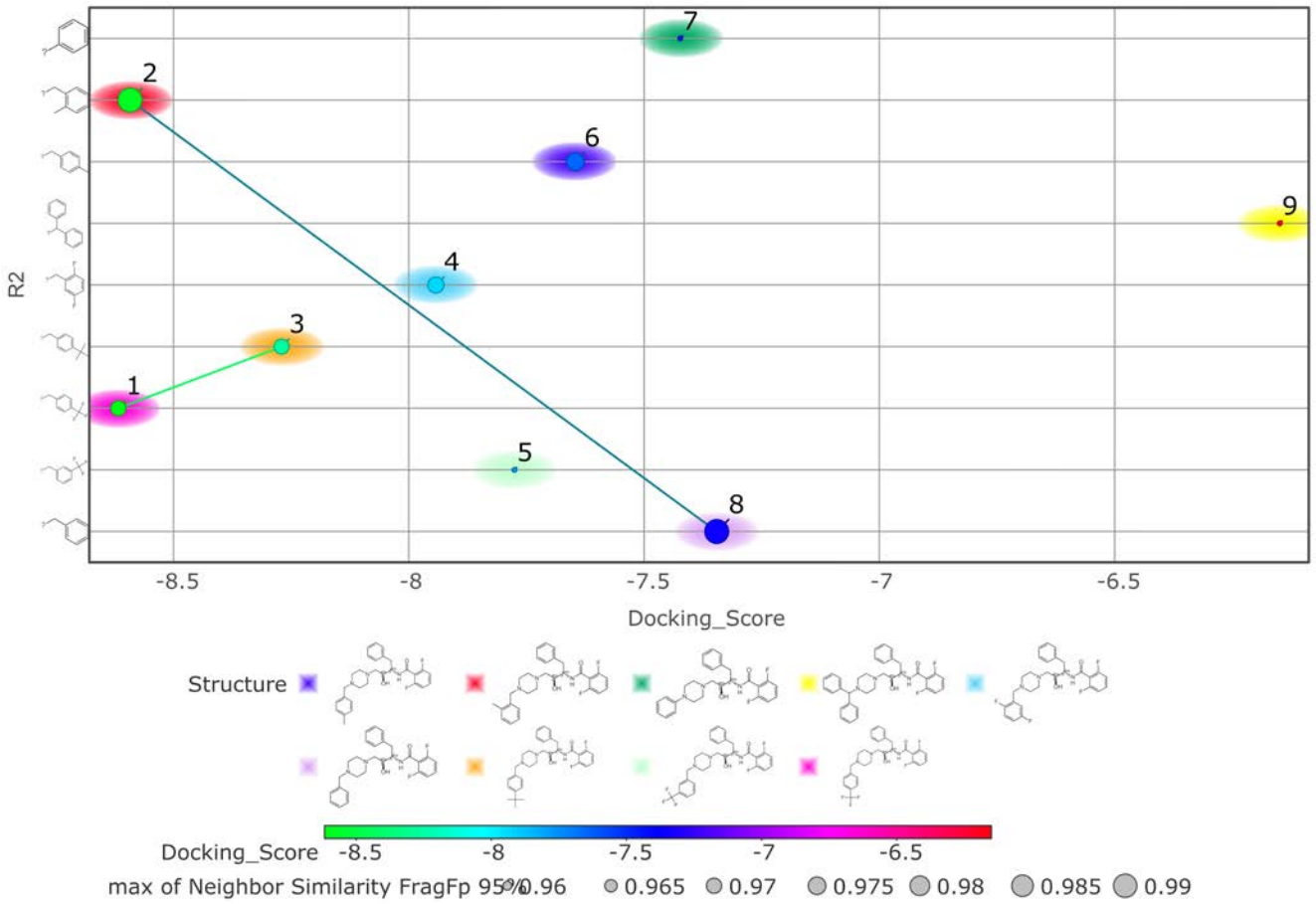

Figure 10: SALI of antiplasmodial compounds having same 2,6-difluorobenzoic acid at pocket I and different substitutions made at pocket II. Antiplasmodial compounds and similarity relationship on the neighbor similarity FragFp-95% as revealed by scattered plot. Compounds arranged according to their docking score and different substitions at R2 The node size variation is the representation of the structurally related compounds while edge reflects the connectivity relationship.

position in compound **20** (-7.566 kcal/mol) showed good effects on docking score than less EDG at para position in compound **30** (-6.918 kcal/mol). The aldehyde group at para position showed better effects on docking score in compound **32** (-6.783 kcal/mol) than hydroxyl group at para position in compound **37** (-6.123 kcal/mol). Compounds **10**, **13**, and **14** possess same Br group at ortho position but meta position varied by presence of -F, -CH_3 and –I group, respectively. It was observed that –CH_3 and –I group has no effect on docking score as both compound **13** (-8.089 kcal/mol) and **14** (-8.025 kcal/mol) have similar docking scores. But strong EWG at ortho position in compound **10** (-8.532 kcal/mol) has a significant effect on docking score compared to compounds **13** and **14**. Compound **12** (-8.096 kcal/mol) showed a better docking score than compound **16** (-7.873 kcal/mol) due to the presence of EWG at both ortho positions compared to EDG at both ortho positions in compound **16**. Compound **24** (-7.422 kcal/mol) and compound **34** (-6.597 kcal/mol) differ by the presence of Br (EWG) and –CH_3 (EDG), respectively. It showed that EWG at meta position has a significant effect of docking score than EDG at the same position.

Conclusion

To determine potent ligands and pharmacophores which are based on rational design and synthesis for target-based, we screened 301 analogs of HEA and piperazine and found hit-compound was a promising hit to target *Pf*Plm I having better docking scores, XP Gscore, and binding free energy than Pepstatin-A. Even MD simulation also suggested good conformational stability of compound over Pepstatin A. During simulation, hit-compound maintained interaction with catalytic residue (Asp32 and Asp215). Finally, it was observed that there was no allosteric site for the hit compound. The potential hit compound is conformationally stable and encouraged us to synthesize and evaluate it for pharmacophore-enzyme interaction.

Supplementary Information

1H NMR Spectrum, 13C NMR Spectrum, Table 1-Listing of HEA-based hit molecules based on docking score (kcal/mol), XP Gscore (kcal/mol) and their free energy as binding energy (kcal/mol) enroute the targeted *Pf*Plm I protein, Table-2 Listing of HEA-based hit molecules based on docking score (kcal/mol),

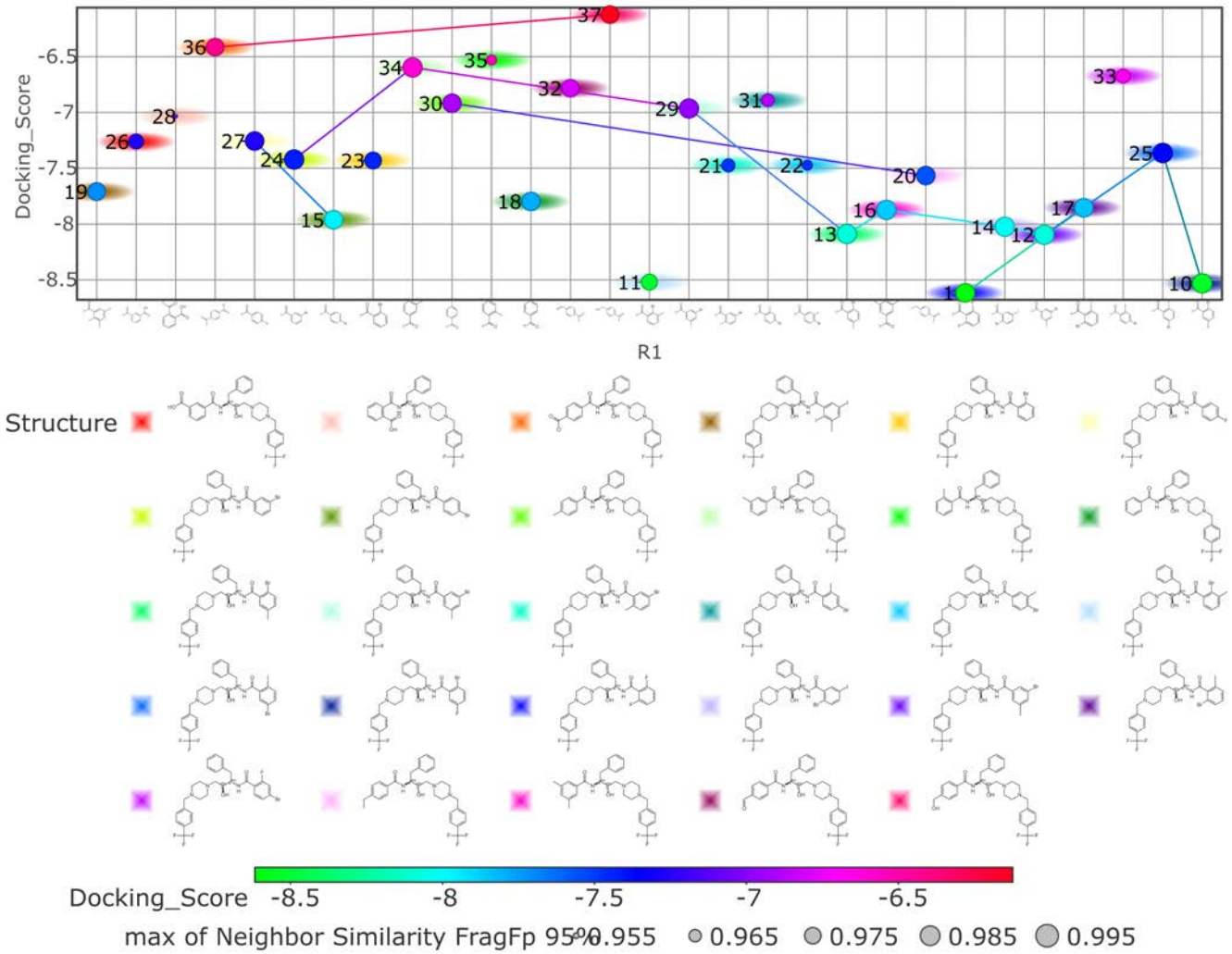

Figure 11: SALI of antiplasmodial compounds having same 4-(trifluoromethyl)benzyl piperazine at pocket II and different substitutions made at pocket I. The similarity relationships amid the antiplasmodial compounds based on the neighbor similarity FragFp-95% as shown by scattered plot. Compounds arranged according to their docking score and different substitions at R1 the node size variation is the representation of the structurally related compounds while connectivity relationships get represents by edge.

XP Gscore (kcal/mol) and their binding free energy (kcal/mol) better than cutoff value (-8.0 kcal/mol) enroute the targeted *Pf*Plm I protein, Table -3, Ramachandran mapping analysis of Stereochemical geometry is reflected in Table -3 for residues of PfPlm I, Table-4 is the study of the relationship between Structure and activity.

Conflict of Interest: Authors declare no conflict of interest.

REFERENCES

1. P. Liu. Plasmepsin: Function, characterization and targeted antimalarial drug development. In: Natural remedies in the fight against parasites; H. F. Khater, M. Govindarajan and G. Benelli, Ed.; Intech: Ezypt, **2017**; pp. 183-218.
2. M.C. Souza, T.A. Padua, N.D. Torres, M.F. Costa, V. Facchinetti, C.R. Gomes, M.V. Souza, M. Henriques. Study of the antimalarial properties of Hydroxyethylamine derivatives using green fluorescent protein transformed Plasmodium berghei. *Mem Inst Oswaldo Cruz* **2015**, 110, 560-565.
3. WHO: World Malaria Report. **2020**.
4. T.N.C. Wells, P.L. Alonso and W.E. Gutteridge. New medicines to improve control and contribute to the eradication of malaria. *Nat. Rev. Drug Discov.* **2009**, 8, 879-891.
5. A.M. Dondorp, F. Nosten, P. Yi et.al. Artemisinin resistance in plasmodium falciparum malaria. *N. Engl. J. Med*. **2009**, 361, 455- 467.
6. R. Banerjee, J. Liu, W. Beatty, L. Pelosof, M. Klemba and D.E. Goldberg. Four plasmepsins are active in the plasmodium falciparum food vacuole, including a protease with an active-site histidine. *PNAS* **2002**, 99, 990-995.
7. J.B. Dame, C.A. Yowell, L. Omara-Opyene, J.M. Carlton, R.A. Cooper, T.Li. Plasmepsin4, the food vacuole aspartic proteinase found in all plasmodium spp. Infecting man. *Molecular and biochemical parasitology* **2003**, 130, 1-12.
8. P. Liu, M.R. Marzahn, A.H. Robbins, H. Gutierrez-de-Teran, D. Rodriguez, S.H. Mcclung, S.M. Stevens, C.A. Yowell, J.B. Dame, R. McKenna etal: Recombinant plasmepsin 1 from the the human malaria parasite plasmodium falciparum: enzymatic characterization, active site inhibitor design, and structural analysis. *Biochemistry* **2009**, 48, 4086-4099.
9. O.A. Asojo, E. Afonina, S.V. Gulnik, B. Yu, J.W. Erickson, R. Randad, D. Madjahed, A.M. Silva: Structures of Ser205 mutant plasmepsin II from

plasmodium falciparum at 1.8 A in complex with the inhibitors rs367 and rs370. *Acta Crystallographica section D, Biological crystallography* **2002**, 58, 2001-2008.
10. O.A. Asojo, S.V. Gulnik, E. Afonina, B. Yu, J.A. Ellman, T.S. Haque, A.M. Sila: Novel uncomplexed and complexed structures of plasmepsin II, an aspartic protease from Plasmodium falciparum. *Journal of molecular biology* **2003**, 327, 173-181.
11. J.C. Clemente, L. Govindsamay, A. Madabushi, S.Z. Fisher, R.E. Moose, C.A. Yowell, K. Hidaka, T. Kimura, Y. Hayashi, Y. Kiso *et* al : Structure of aspartic protease plasmepsin 4 from the malarial parasite Plasmodium malariae bound to an allophenylnorstatine-based inhibitor. *Acta crystallographica Section D, Biological Crystallography* ***2006,*** 62, 246-252.
12. A.M. Silva, A.Y. Lee, S.V. Gulnik et.al. Structure and inhibition of plasmepsin ii, a hemoglobin-degrading enzyme from plasmodium falciparum. *PNAS* **1996,** 93, 10034-10039.
13. S.E. Francis, R. Banerjee, D.E. Goldberg: Biosynthesis and maturation of the malaria aspartic hemoglobinases plasmepsin I and II. *J. Biol. Chem.* **1997**, 272, 4961-14968.
14. S.E Francis, I.Y. Gluzman, A. Oksman, A. Knickerbocker, R. Mueller, M.L. Bryant, D.R. Sherman, D.G. Rusell, D.E. Goldberg: Molecular characterization and inhibition of plasmodium falciparum aspartic hemoglobinase. *The EMBO journal* **1994**, 13, 306-317.
15. E. Bailly, R. Jambou, J. Savel, G. Jaureguiberry. Plasmodium falciparum: Differential sensitivity in vitro to E-64 (Cysteine Protease Inhibitor) and Pepstatin A (Aspartyl Protease Inhibitor). *J. Protozoology*, **1992**, 39(5), 593-599.
16. R.P. Moon, L. Tyas, U. Certa, K. Rupp, D. Bur, C. Jacquet, H. Matile, H. Loetscher, F. Grueninger-Leitch, J. Kay etal. Expression and characterization of plasmepsin I from Plasmodium falciparum. *European journal of biochemistry* **1997**, 244, 552-560.
17. A.K. Singh, V. Rajendran, S. Singh et.al. Antiplasmodial activity of hydroxyethylamine analogs: Synthesis, biological activity and structure activity relationship of plasmepsin inhibitors. *Bioorg. Med. Chem***. 2018**, 26, 3837-3844.
18. S. Singh, V. Rajendran, J. He, A.K. Singh, A.O. Achieng, A. Pant. Vandana, A.S. Nasamau, M. Pandit, J. Singh et al. Fast acting molecules targeting malarial aspartic proteases, plasmepsin, inhibit, malaria infection at multiple stages. *ACS Infectious Diseases* **2019**, 5, 184-198.
19. B. Rathi, P.P. Sharma, R.P. Singh. Tetrahedral Hydroxyethylamine: A privileged scaffold in development of antimalarial agents. *Chemical biology letters*. **2014**, 1(1), 11-13.
20. S. Schrödinger Release 2020-1: Protein Preparation Wizard; Epik, LLC, New York, NY, 2020; Impact, Schrödinger, LLC, New York, NY; Prime, Schrödinger, LLC, New York, NY, **2020.**
21. https://pubchem.ncbi.nlm.nih.gov/compound/5478883 (accessed on July 15).
22. H. Xiao, T. Tanaka, M. Ogawa, R.Y. Yada. Expression and enzymatic characterization of the soluble recombinant plasmepsin I from plasmodium falciparum. *Protein engineering, design & selection*. **2007**, 20, 625-633.
23. Schrödinger Release 2020-1: Maestro, Schrödinger, LLC, New York, NY, **2020.**
24. S. Kumar, C. Upadhyay, M. Bansal, M. Grishina, B.S. Chhikara, V. Potemkin, B. Rathi and Poonam. Experimental and computational studies of microwave-assisted, facile ring opening of epoxide with less reactive aromatic amines in nitromethane. *ACS omega* **2020**, 5, 18746-18757.
25. K.E.B. Parkes, D.J. Bushnell, P.H. Crackett et.al. Studies toward the large-scale synthesis of the hiv proteinase inhibitor ro 31-8959. *J. Org. Chem*. **1994**, 59, 3656-3664.
26. M. Stefanidou, C. Herrera, N. Armanasco and R.J. Shattock. Saquinavir inhibits early events associated with establishment of hiv-1 infection: Potential role for protease inhibitors in prevention. Antimicrob. *Agents Chemother*. **2012**, 56, 4381-4390.
27. Schrödinger Release 2020-1: LigPrep, Schrödinger, LLC, New York, NY, **2020**.
28. Schrödinger Release 2020-1: Epik, Schrödinger, LLC, New York, NY, **2020.**
29. Schrödinger Release 2020-1: Glide, Schrödinger, LLC, New York, NY, **2020**.
30. Schrödinger Release 2020-1: Prime, Schrödinger, LLC, New York, NY, **2020**.
31. K.J. Bowers, E. Chow, H. Xu, R.O. Dror, M.P. Eastwood, B.A. Gregersen, J.L. Klepeis, I. Kolossvary, M.A. Moraes, F.D. Sacerdoti, J.K. Salmon, Y. Shan and D.E. Shaw. Scalable algorithms for molecular dynamics simulations on commodity clusters. In, Proceedings of the 2006 ACM/IEEE conference on Supercomputing. Tampa, Florida: *Association for Computing Machinery*. **2006**. p. 84–es.
32. Schrödinger Release 2020-1: Desmond Molecular Dynamics System, D. E. Shaw Research, New York, NY, 2020. Maestro Desmond Interoperability Tools, Schrödinger, New York, NY, **2020**.
33. W.L. Jorgensen and J. Tirado-Rives. The opls [optimized potentials for liquid simulations] potential functions for proteins, energy minimizations for crystals of cyclic peptides and crambin. *J. Am. Chem. Soc*. **1988**, 110, 1657-1666.
34. W.L. Jorgensen, D.S. Maxwell and J. Tirado-Rives. Development and testing of the opls all-atom force field on conformational energetics and properties of organic liquids. *J. Am. Chem. Soc*. **1996**,118, 11225-11236.
35. W.L. Jorgensen, J. Chandrasekhar, J.D. Madura, R.W. Impey and M.L. Klein. Comparison of simple potential functions for simulating liquid water. *J. Chem. Phys.* **1983**, 79, 926-935. DOI: 10.1063/1.445869.
36. G.J. Martyna, D.J. Tobias and M.L. Klein. Constant pressure molecular dynamics algorithms. *J. Chem. Phys*. **1994**, 101, 4177- 4189.
37. S. Nosé. A unified formulation of the constant temperature molecular dynamics methods. *J. Chem. Phys.* **1984**, 81, 511-519.
38. R.A. Laskowski, M.W. MacArthur, D.S. Moss and J.M. Thornton. Procheck: A program to check the stereochemical quality of protein structures. *J. Appl. Cryst*. **1993**, 26, 283-291.
39. S. Dallakyan and A.J. Olson. Small-molecule library screening by docking with pyrx. In: Chemical biology: Methods and protocols; Hempel, J.E., Williams, C.H. and Hong, C.C., Ed.; *Springer New York: New York*, NY, **2015**; pp. 243-250.
40. Schrodinger, LLC. The pymol molecular graphics system, version 1.8. In.; **2015**.
41. A. Daina, O. Michielin and V. Zoete. Swissadme: A free web tool to evaluate pharmacokinetics, drug-likeness and medicinal chemistry friendliness of small molecules. *Sci. Rep*. **2017,** 7, 42717.
42. P.M. Cheuka, G. Dziwornu, J. Okombo and K. Chibale. Plasmepsin inhibitors in antimalarial drug discovery: Medicinal chemistry and target validation (2000 to present). *J. Med. Chem*. **2020**, 63, 4445–4467.